

Akiyoshi Kakita · Shintaro Hayashi · Francesca Moro · Renzo Guerrini · Tsunenori Ozawa · Koji Ono
Shigeki Kameyama · Christopher A. Walsh · Hitoshi Takahashi

Bilateral periventricular nodular heterotopia due to *filamin 1* gene mutation: widespread glomeruloid microvascular anomaly and dysplastic cytoarchitecture in the cerebral cortex

Received: 6 August 2001 / Revised: 12 June 2002 / Accepted: 12 June 2002 / Published online: 23 July 2002
© Springer-Verlag 2002

Abstract Bilateral periventricular nodular heterotopia (BPNH) is a neuronal migration disorder that is characterized by subependymal nodules of gray matter. Recently, a causative gene for BPNH, *filamin 1*, has been identified, and possible roles of the translated protein in cell migration and blood vessel development have been proposed. We report here the histopathological features of an autopsy case of BPNH with widespread glomeruloid microvascular anomaly and dysplastic cytoarchitecture in the cerebral cortex, in whom we found a novel exon 11 (Val528Met) *filamin 1* mutation. Within the periventricu-

lar nodules, well-differentiated pyramidal neurons were randomly oriented. A small proportion of neurons were immunolabeled with antibodies raised against calbindin D-28k, parvalbumin, or calretinin. We used a carbocyanine dye (DiI) tracing technique to investigate the extent of fiber projections within and outside the nodules. The labeled fibers formed bundles that extended into the surrounding white matter. Connections between adjacent nodules were evident. Connections between the nodules and the cerebral cortex were also seen, with a small number of labeled fibers reaching the cortex. In the cerebral cortex, small closely packed vessels ran in a parallel fashion throughout all of the layers. Immunohistochemically, the inner rim of individual vessel lumina was labeled by an antibody against factor VIII, and the vessel walls were labeled by antibodies against actin and laminin. Astrocyte processes, labeled with an antibody to glial fibrillary acidic protein, invaded these vascular channels. Ultrastructurally, a network of basal lamina-like materials lined with endothelial cells was evident. The cytoarchitecture of the cerebral cortex was disturbed, in that the columnar neuronal arrangement was distorted around the malformed vessels. This case appears to represent an example of BPNH manifesting widespread developmental anomalies within the blood vessels and the cortical cytoarchitecture in the cerebrum.

A. Kakita · S. Hayashi · H. Takahashi
Department of Pathology, Brain Research Institute,
Niigata University, 1 Asahimachi, Niigata 951-8585, Japan

A. Kakita (✉)
Department of Pathological Neuroscience,
Resource Branch for Brain Disease Research,
Center for Bioresource-based Research, Brain Research Institute,
Niigata University, 1 Asahimachi, Niigata 951-8585, Japan
e-mail: kakita@bri.niigata-u.ac.jp,
Tel.: +81-25-2270673, Fax: +81-25-2270817

F. Moro
Neurogenetics Laboratory, DUNPI-IRCCS Fondazione Stella Maris,
Via dei Giacinti 2, Pisa, Italy

R. Guerrini
Neurosciences Unit,
Institute of Child Health
and Great Ormond Street Hospital for Children,
University of College London,
The Wolfson Centre, Mecklenburgh Square, London, UK

T. Ozawa · K. Ono
Department of Neurosurgery, Niigata Chuo Hospital,
1-18 Shinko-chou, Niigata, Japan

S. Kameyama
Department of Neurosurgery, National Epilepsy Center,
Nishi-Niigata Central Hospital, 1 Masago, Niigata, Japan

C.A. Walsh
Division of Neurogenetics, Department of Neurology,
Beth Israel Deaconess Medical Center,
Harvard Institute of Medicine, 77 Avenue Louis Pasteur, Boston,
Massachusetts, USA

Keywords *Filamin 1* · Migration disorder · Epilepsy · Vascular anomaly · Subependymal heterotopia

Introduction

Bilateral periventricular nodular heterotopia (BPNH) is a neuronal migration disorder that is characterized by subependymal gray matter nodules. The X-linked dominant inheritance pattern for BPNH is one of the most characterized syndromes, where the majority of patients with BPNH are female [2, 11, 12, 27, 28, 36, 37] and most males with the underlying gene mutations die during early embryogenesis [11]. A large proportion of patients suffer from seizures that begin in the second or third decade of

life [2, 8, 12, 27, 36, 37] and some suffer strokes at a young age [16]. In addition to BPNH, other anomalies, within and outside the CNS, have been observed in patients, including hypoplasia of the corpus callosum [2, 7, 8, 9, 16, 36], mild cerebellar hypoplasia [2, 9, 16, 33], and patent ductus arteriosus [16, 36].

Linkage analysis for BPNH mapped this disorder to Xq28 [12], and the gene was subsequently identified as the *filamin 1* gene [16]. The encoded protein, FLN1, is also known as actin-binding protein 280 (ABP-280) [19, 21, 22, 23], which is known to play a critical role in the control of cell shape, migration, filopodia formation, and chemotaxis [30]. A high level of FLN1 expression has been found in neurons of the developing cortex, and it is subsequently down-regulated in the adult, implying a role in neuronal migration [12, 16].

Several neuroimaging studies have been performed to investigate BPNH, and its characteristics have been reported [2, 36, 43]. On the other hand, there are few histological descriptions of the tissue [11, 12, 43] and no histopathological description of a genetically proven FLN1 mutation. Recently, we studied an autopsy case of a female with BPNH, in whom widespread glomeruloid microvascular anomalies and associated dysplastic cytoarchitecture in the cerebral cortex were evident. Here we describe the histopathological features, and report the fiber extensions within and outside the nodules as examined using a carbocyanine dye (DiI) tracing technique. Furthermore, we carried out single-strand conformation polymorphism (SSCP) mutation analysis of the *FLN1* gene, and identified a novel exon 11 (Val528Met) mutation.

Patient and methods

Clinical history and autopsy findings

The patient, a Japanese woman, was born at full term with a patent ductus arteriosus that was surgically corrected at the age of 14 years. Her first seizure was noted at 16 years of age and was characterized by unsteadiness and consciousness impairment. This was followed by frequent simple and complex partial seizures, despite treatment with anti-epileptic drugs. Her interictal electroencephalogram showed bilateral frontotemporal polyspikes, sharp waves and bursts of high-voltage slow waves. A brain MRI study revealed heterotopic gray matter lining the walls of the lateral ventricles (Fig. 1A) and hypoplasia of the splenium of the corpus callosum (Fig. 1B). Although formal psychometric tests were not performed, she had been judged as mildly mentally retarded. She was a junior high school graduate, and was unemployed and unmarried. She had no family history of neurological disease.

At the age of 48 years, she was unfortunately struck by a motorbike. On admission to hospital, she was alert and showed no neurological symptoms. X-ray examination indicated fractures of the right tibia, fibula, and the fifth metatarsus. However, the next morning she showed sudden and severe disturbances of consciousness without seizure activity, after which tetraplegia and respiratory disturbance developed. On the 3rd day after sustaining the injury the patient died.

At autopsy, the fresh brain weighed 1,540 g, showing severe swelling with uncal and tonsillar herniations. Fresh ischemic changes were observed throughout the brain. The brain, spinal cord, and visceral organs were fixed with 20% phosphate-buffered formalin for histological examination. In the histology sections, staining with Sudan-III lipid stain revealed the presence of fat droplets within

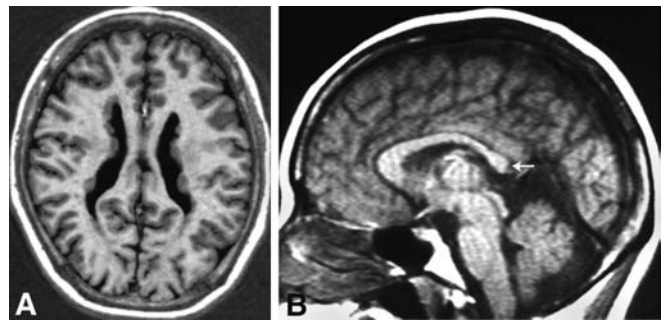


Fig. 1A, B T1-weighted magnetic resonance images of the brain. **A** An axial image demonstrates multiple nodules of heterotopic gray matter lining the walls of both lateral ventricles. **B** A sagittal image shows hypoplasia of the splenium of the corpus callosum (arrow)

the lumen of multiple blood vessels in both lungs, and in the liver and brain: the cause of her death was considered to be fat embolism.

Histological procedures

The cerebral hemispheres were sectioned coronally, and the brain stem, cerebellum, and spinal cord were sectioned transversely. We identified periventricular nodules in the cerebrum (described below). From the paraffin-embedded block samples, serial 4- μ m-thick sections were cut and stained with hematoxylin and eosin, Klüver-Barera method, Bodian's method, and the van Gieson stain for elastin.

Immunohistochemical studies were performed on the formalin-fixed, paraffin-embedded sections using the avidin-biotin-peroxidase complex (ABC) method, with the Vectastain ABC kit (Vector, Burlingame, Calif.). The following primary antibodies were used: rabbit polyclonal antibodies against glial fibrillary acidic protein (GFAP; Dako, Glostrup, Denmark; diluted 1:1,000); actin (Advance, Tokyo, Japan; 1:400); calretinin (Chemicon, Temecula, Calif.; 1:200); and laminin (Dako; 1:1,600), and mouse monoclonal antibodies against the phosphorylated epitope of neurofilament (SMI-31; Sternberger Monoclonal, Lutherville, Md.; 1:5,000); type IV collagen (Advance; 1:100); factor VIII (Dako; 1:250); calbindin D-28k (Sigma Chemical, St. Louis, Mo.; 1:400); and parvalbumin (Sigma; 1:500). The chromogen reaction was developed with 0.02% diaminobenzidine (Wako Chemical, Tokyo, Japan) and 0.05% H_2O_2 in 0.05 M TRIS-HCl buffer, pH 7.6, for 10 min.

For electron microscopy, formalin-fixed tissue fragments from the frontal cortex were used. The fragments were post-fixed with 1% osmium tetroxide, dehydrated through a graded ethanol series and embedded in Epon 812 resin. Ultrathin sections were cut and stained with uranyl acetate and lead citrate, and examined with a Hitachi H7100 electron microscope at 75 kV.

DiI tracing study

To investigate the connectivity between heterotopic nodules and to trace fiber projection from the nodules, we applied a DiI tracing technique using formalin-fixed, 1-cm-thick coronal slices taken at the level of the thalamus. A small number of DiI crystals [DiIC₁₈ (3), Molecular Probes, Eugene, Ore.] were placed on the cut-surface of the periventricular nodules on two slices; on another two slices, we put the DiI on the white matter adjacent to the nodules. The slices were left in a humidified dark chamber at 37°C for 5 months. Serial semithin sections, 100 μ m thick, were then cut on a Vibratome (Leica VT1000S, Nussloch, Germany), and collected in PBS. The lipophilic tracer-labeled fibers were viewed using an Olympus AX80T (Tokyo, Japan) microscope equipped with epifluorescence optics. The images were captured by a digital camera (DP50; Olympus), and then transferred onto a Power Macintosh G4, and processed using Adobe Photoshop 6.0 software.

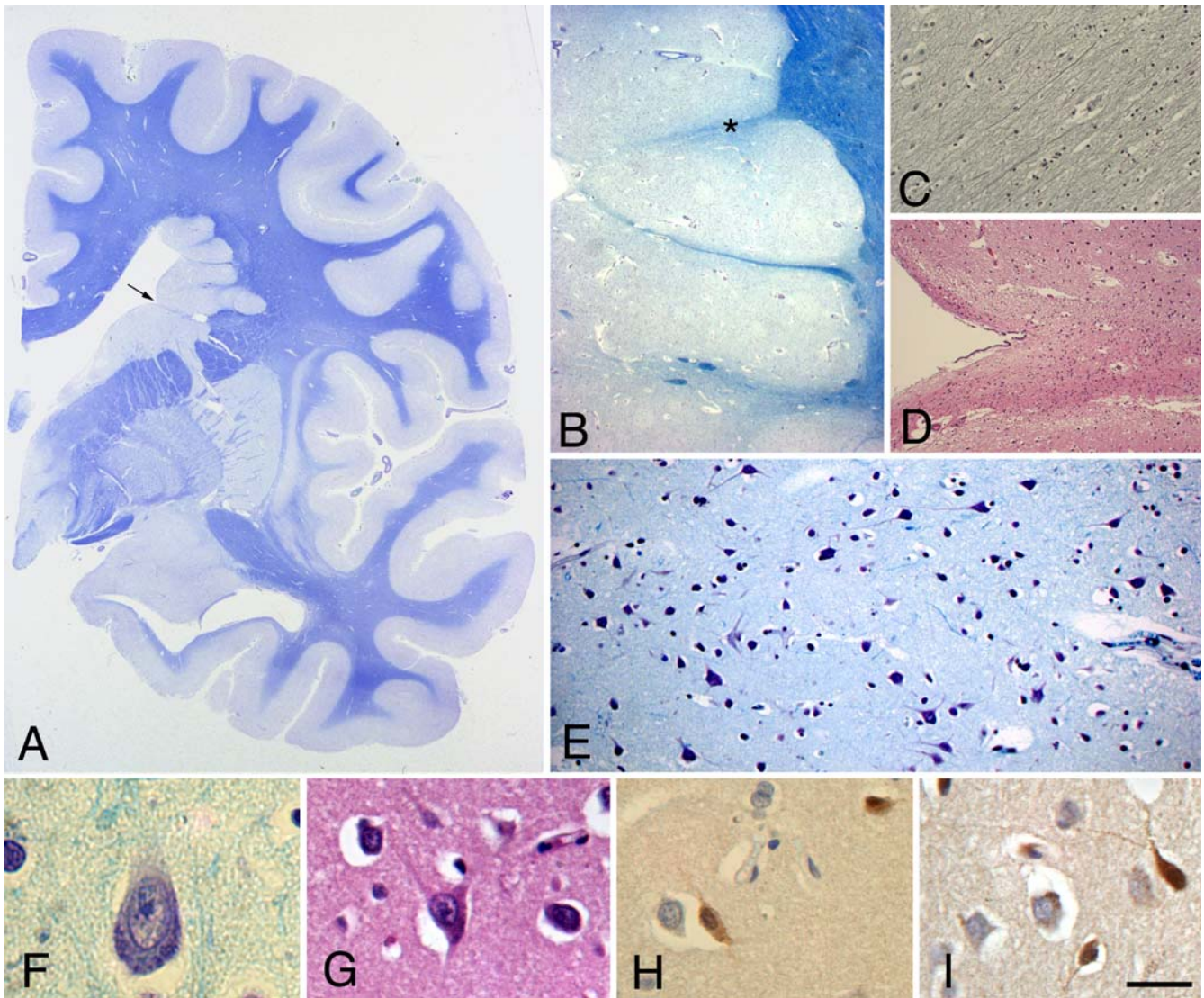


Fig. 2A–I Periventricular nodular heterotopia. **A** A coronal section of the right cerebral hemisphere through the basal ganglia, showing heterotopic nodules of gray matter at the lateral angle of the lateral ventricle. **B** Higher magnification view of the heterotopic nests. A few linear bundles of myelinated fibers of the white matter are seen within the nest. **C** The same area as indicated by an asterisk in **B**. Argyrophilic axon fibers are evident in the bundles. **D** The border between the heterotopic nodule (upper part) and the caudate nucleus (lower part), as indicated by an arrow in **A**. A thin white matter bundle separates the nodule and the caudate nucleus, and reaches to the ventricular surface. **E** Within the nodules, well-differentiated pyramidal neurons showing variable orientations of the apical dendrites are seen. **F, G** Examples of neurons within the nodules. Relatively large nuclei with prominent nucleoli, and pyramidal-shaped cell bodies with some dendrites are seen. **H** The cytoplasm of two neurons is labeled by anti-calbindin antibody. **I** The cytoplasm and processes of two neurons are labeled by anti-calretinin antibody. **A, B, E, F** Klüver-Barrera (K-B) stain; **C** Bodian's method; **D, G** hematoxylin and eosin (H&E) stain; **H, I** immunostaining and counterstaining with hematoxylin. *Bar* **A** 7.5 mm; **B** 1.3 mm; **C** 100 μ m; **D** 220 μ m, **E** 50 μ m, **F** 15 μ m, **G–I** 20 μ m

Mutational analysis

For gene analysis, we took a piece of the fresh spinal cord at autopsy and stored it at -80°C before performing SSCP analysis of all 48 coding exons of *FLNI* gene as described elsewhere [32]. In brief, genomic DNA was extracted from the frozen tissue; each exon was then amplified by polymerase chain reaction (PCR) and purified using the QIAquick PCR purification kit (QIAGEN spa, Milan, Italy). The PCR products were run on the SSCP gels, and analyzed by direct sequencing using BigDye Terminator chemistry (ABI PRISM 310; Applied Biosystem, Foster City, Calif.).

Results

Periventricular heterotopia

The histological features of periventricular heterotopia were studied in several coronal slices. The heterotopia were discontinuous in the rostrocaudal axis, showing multiple nodules of variable size. They were located bilaterally, adjacent to the frontal horns, trigones, bodies, and occipital horns of the lateral ventricles, and just dorsal to the caudate nucleus (Fig. 2A). The boundaries between the nodules

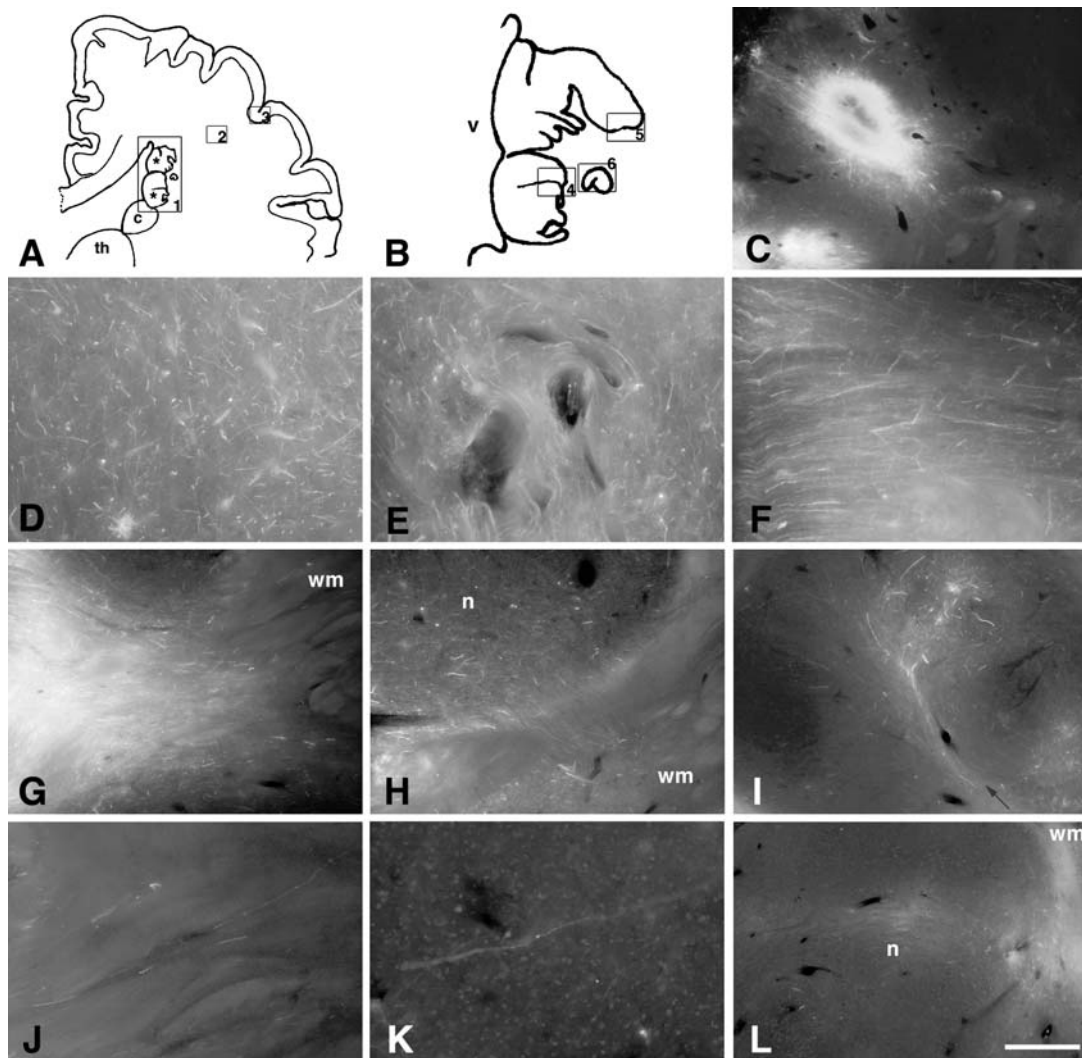


Fig. 3A–L DiI labeling of fibers within and outside the heterotopic nodules. **A** A schematic drawing of an example of slices used in the DiI tracing study. Two *stars* indicate the approximate positions of crystal placement on the surface of the nodules (*c* caudate nucleus, *th* thalamus). **B** A detailed schematic drawing of the area indicated by *square 1* in **A**. There are two relatively large nodules (*upper* and *lower*) separated by a thin white matter bundle, and a small island (*right*) (*v* lateral ventricle). **C** A position of crystal placement showing intense labeling, from which radially oriented labeled fibers extend. **D** Within nodules the individual fibers run in an undirected manner. **E** Around the blood vessels (dark, elongated circles), the fibers are curved. **F** A part close to the white matter where fibers run in a parallel fashion. **G** The area indicated by *square 4* in **B**. The fibers extend from the nodule (*left*) into the white matter (*wm*) through a linear indentation of myelinated fibers. **H** The area indicated by *square 5* in **B**. Some fibers extend across the margin of the nodule (*n*) into the surrounding white matter (*wm*). **I** The area indicated by *square 6* in **B**. A small number of labeled fibers penetrate another heterotopic nodule in a parallel fashion through a linear indentation (*arrow*). After getting into the nodule, they run in a random manner (*upper*). **J** The area indicated by *square 2* in **A**. A single, labeled fiber is seen in the deep white matter. **K** The area indicated by *square 3* in **A**. A single, labeled fiber is seen in the cortex. **L** Fibers in another slice, with crystals placed on the white matter rather than within the nodules. The fibers extend from the white matter (*wm*) into the nodule (*n*). *Bar* **C** 1.2 mm; **D** 45 μ m; **E** 20 μ m; **F** 25 μ m; **G** 120 μ m; **H** 300 μ m; **I** 600 μ m; **J**, **K** 18 μ m; **L** 500 μ m

and the adjacent white matter were clear, but some linear bundles of myelinated fibers invaded the nodules (Fig. 2B). The myelinated bundles contained argyrophilic axon fibers (Fig. 2C), which were labeled by an antibody against the phosphorylated epitope of neurofilament (SMI-31, data not shown). At the border between the heterotopic nodules and the caudate nucleus, a thin line of myelinated fibers ran into the nodules and reached the ventricular surface (Fig. 2D). The heterotopic nodules contained well-differentiated neurons with variable orientations of the apical dendrites (Fig. 2E). Medium to large pyramidal neurons, with large pale-staining nuclei, prominent nucleoli, and apical and basal dendrites, were mainly observed (Fig. 2F, G). A few small neurons were also seen scattered throughout the nodules. The histological character of the neurons were more similar to those of the cerebral cortical neurons, rather than neurons in the caudate nucleus. Immunohistochemically, a small proportion of small neurons within the nodules were labeled by antibodies against calbindin D-28k (Fig. 2H), parvalbumin, or calretinin (Fig. 2I), where estimated percentages of the immunolabeled neurons by any of the three antibodies were less than 1% of the total neuron population within the nodules. Astrocytes and

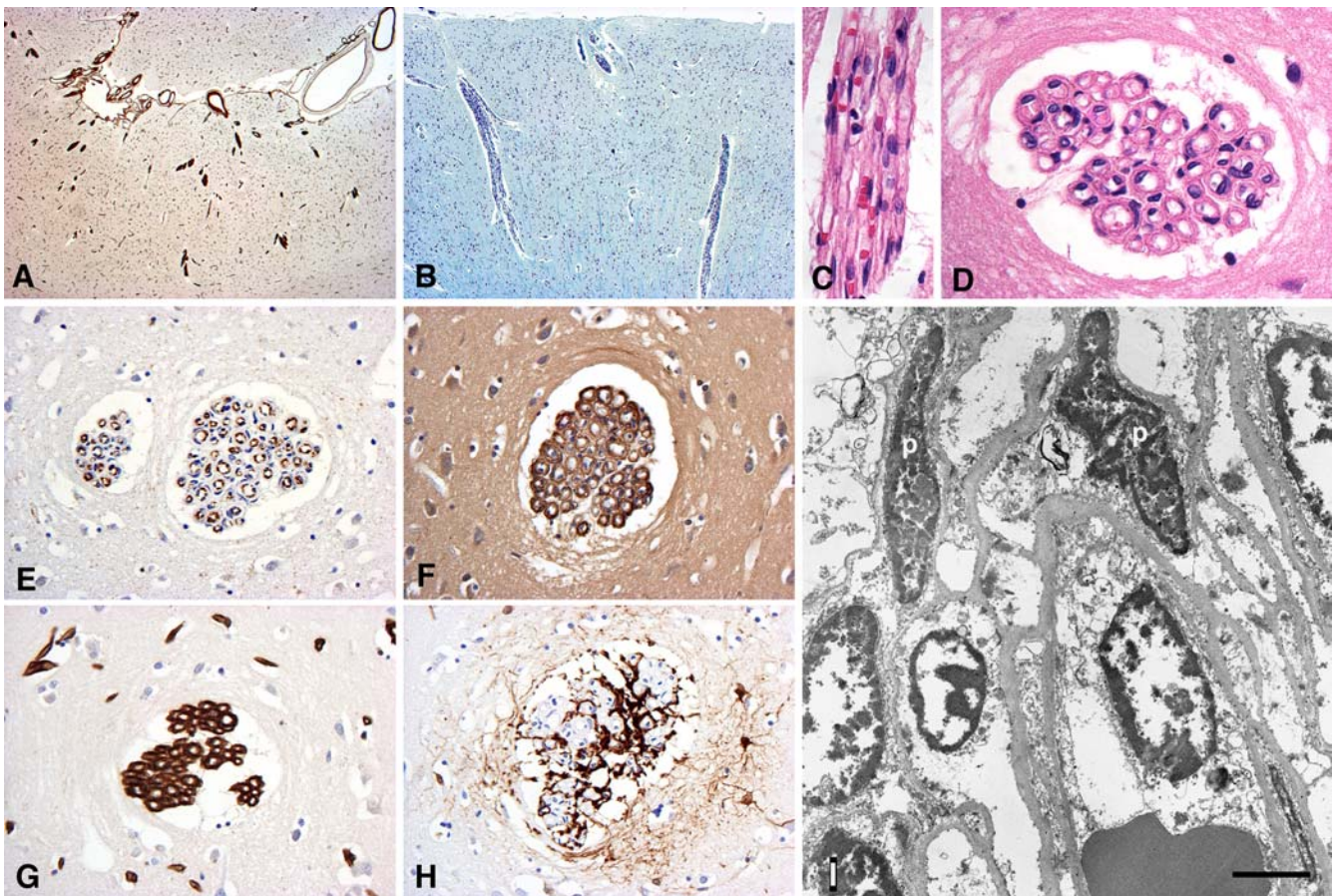


Fig. 4A–I Glomeruloid microvascular changes in the cerebral cortex. **A** A widespread distribution of the abnormal vessels is demonstrated by laminin immunohistochemistry. *Black dots* in the cortex represent the immunolabeled glomeruloid vessels. **B** Longitudinally cut vessels within the Virchow-Robin space lie in the cortex, indicating an increased number of cellular elements. **C** A cluster of longitudinally cut vessels. The individual vessel runs in a parallel fashion. **D** In a cross-section, the cluster is seen as a tufted collection of capillary-like small vessels. **E** Immunohistochemistry using an antibody against factor VIII demonstrates a thin immunopositive rim covering the inner surface of individual lumina of the vessels. **F** The walls of the vessels are labeled by an anti-actin antibody, with variable intensity. **G** The walls are strongly labeled by an anti-laminin antibody. **H** GFAP-labeled processes of astrocytes are seen within the channels of vessel walls. **I** An electron micrograph of the vessels demonstrates a network of basal lamina-like electron-dense material. Endothelial cells bounding the lumen, and pericytes (*p*) are seen. **A–I** Frontal cortex. **A, E–H** Immunostaining and counterstaining with hematoxylin; **B** K-B stain; **C, D** H&E stain. *Bar* **A** 1.2 mm; **B** 500 μ m; **C** 25 μ m; **D** 20 μ m; **E–H** 40 μ m; **I** 2.5 μ m

oligodendroglia were also evident within the nodules. Several abnormal vessels showing glomeruloid changes (described below) were observed within the nodules.

The size of the ventricles was normal. We did not observe changes consistent with mesial temporal sclerosis, which includes loss of pyramidal neurons and astrogliosis in the hippocampal formation, and has been reported in patients with intractable epilepsy [47] or with periventricular heterotopia [37, 41].

Using the DiI tracing technique, we investigated the extent of fiber projection within and outside the nodules.

Small amounts of DiI crystal were placed onto the surface of the heterotopic nodules (Fig. 3A), which consisted of two relatively large nodules separated by a thin white matter bundle and a small island of heterotopic gray matter in the overlying white matter (Fig. 3B). At the locations of the crystal the labeling was intense, and from there the labeled fibers extended radially (Fig. 3C). In most fields within the nodules, the individual fibers ran in an undirected manner (Fig. 3D), and they curved close to blood vessels (Fig. 3E). In some regions they tended to run in a parallel fashion (Fig. 3F), forming bundles that extended into the surrounding white matter (Fig. 3G). At the boundaries of the nodules and the white matter, some fibers extended directly across the margin of the nodules rather than through the white matter bundles (Fig. 3H). Some of these fibers entered other nodules in a parallel fashion via myelinated indentations of the white matter, and ran randomly after entering the nodule (Fig. 3I). We also identified a small number of labeled fibers in the deep white matter separate from the nodules (Fig. 3J), and in the cortex lateral to the nodules (Fig. 3K), indicating that some of the fibers that originated in the nodules run through the white matter to reach to the cortex. We did not encounter labeled fibers within the white matter or the cortex (dorsal to the nodules), or in the internal capsule. We also confirmed fiber connections between the white matter and the nodules by applying DiI crystals onto the surrounding white matter, rather than within the nodules, in other slices. In these slices some labeled fibers were also found within the nodules (Fig. 3L).

Abnormal vessels and cortical dysplasia

Anomalies of the blood vessels were widespread and found both within and outside the periventricular nodules. Outside the nodules the vessels exhibited features of glomeruloid microvascular anomalies, and were seen mainly in the cerebral cortex where they were distributed through all layers (Fig. 4A). Most arteries in the subarachnoid space looked normal, but several longitudinally cut vessels within the Virchow-Robin space showed abnormal features, with some closely packed, small vessels running in a parallel fashion (Fig. 4B, C). Red blood cells were observed within many of the individual lumina (Fig. 4C). In cross-sections, the vessels were arranged as a tufted collection of multiple small lumina separated by circular walls (Fig. 4D). The elastic lamellae or tunica media proper were not observed. The diameter of the vessel lumina was small as for capillaries, but the walls were thicker than those of normal capillaries. Immunohistochemically, an antibody against factor VIII demonstrated a thin immunopositive rim of endothelial cells covering the inner surface of each lumen (Fig. 4E). The walls of vessels were labeled by anti-actin antibody with variable intensity (Fig. 4F). The walls of the vessel channels were also labeled by anti-laminin (Fig. 4G) and anti-collagen type IV antibodies. Processes of the astro-

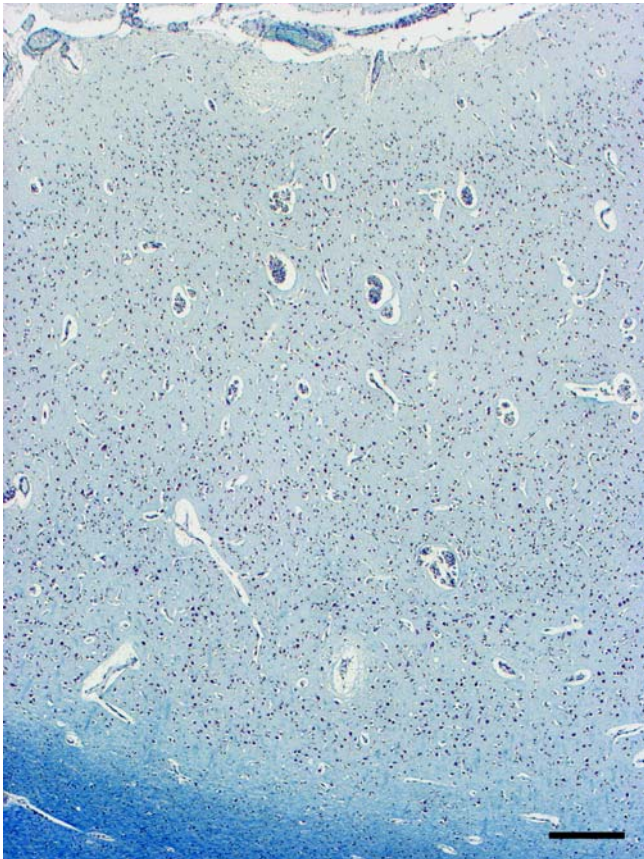


Fig. 5 Light micrograph of all of the layers of the frontal cortex. The cytoarchitecture of the cortex seems to be disturbed around the glomeruloid vessels. K-B stain. Bar 250 μ m

cytes, labeled by a GFAP antibody, invaded irregularly into the channels (Fig. 4H). Ultrastructurally, a network of basal lamina-like electron-dense materials of variable thickness encircled the vessel lumina (Fig. 4I). There were endothelial cells with relatively pale nuclei bounding the lumen. Some pericytes with elongated, dark nuclei were also observed close to the walls. In the cerebrum, the abnormal vessels were frequently observed in the frontal and occipital cortices, and less frequently in the temporal cortex. Such vessels were rarely encountered in the white matter. Within the periventricular heterotopic nodules, many vessels showed similar features. We also observed a small number of abnormal vessels in the basal ganglia, thalamus, brain stem, and cerebellum, although they occurred less frequently than in the cerebral cortex.

The thickness of the cerebral cortex, both dorsal and lateral to the periventricular nodules, did not appear to be reduced. The cortex showed widespread disturbance of the cytoarchitecture; notably the columnar arrangement of neurons was distorted around the vessels so that the neurons appeared to be distributed irregularly (Fig. 5). This feature was most evident in the frontal cortex. We considered these features as a form of dysplasia associated with the microvascular anomaly.

Mutation of *FLN1* gene exon 11

SSCP and DNA sequence analysis of the *FLN1* gene revealed a heterozygous base pair change in one allele at nucleotide 1582 (G to A) in exon 11, resulting in a Val to

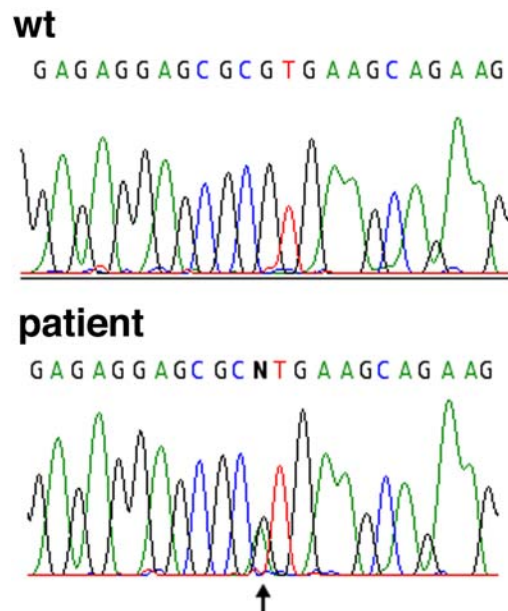


Fig. 6 *FLN1* gene mutation in the patient. Electropherogram of the genomic PCR products corresponding to exon 11 taken from a normal control (*wt*) and the patient. A heterozygous mutation is detected at cDNA position 1582 G to A (GTG to ATG), resulting in the amino acid change V528M. Sequencing was performed using a sense primer

Met substitution at amino acid position 528 in the protein (Fig. 6). This change was located within the third repeat of the ROD domain. This substitution was not found in the 100 unrelated control individuals (data not shown).

Discussion

Neuronal migration defects are manifested in a variety of ways, which may result in heterotopia at variable locations along the migration pathways [3, 17]. Periventricular heterotopia is seen in several conditions, and there are likely to be multiple causative genes [2] or other etiological factors. A few male individuals with bilateral or unilateral periventricular heterotopia have been reported [4, 8, 10, 11, 13, 27, 29, 41, 42, 43]. However, mutations in the *FLNI* gene appear to be the most common cause of familial BPNH [15], and protein truncations or splicing mutations tend to affect the N terminus of the protein encoded by the first 6 of the 48 coding exons (numbered as exons 2–8) [16, 40]. Recently, SSCP analysis of *FLNI* throughout its entire coding region has revealed mutations in the gene in sporadic female and male patients with BPNH [40] and familiar cases [32]. In the sporadic case presented here, we performed SSCP analysis using the frozen tissue obtained at autopsy, and identified a novel point mutation at exon 11 of *FLNI*. This G to A substitution changes a Val to Met at amino acid 528, in the ROD domain. It is unknown whether this mutation results in a stable, mutated protein or whether the mutation disrupts mRNA or protein stability and behaves as a null allele. Although some other missense mutations (for example, an exon 13 mutation causing a L656F substitution in a male [40]) appear to behave as partial loss of function mutations, the clinical and radiological characteristics of our patient, including the intractable epilepsy, patent ductus arteriosus, and hypoplasia of the splenium of the corpus callosum resemble the features of other females with severe loss of function mutations. Since our patient had no known pregnancies, it is not known whether the V528M substitution would be lethal to males. However, this case represents the first autopsy report of a BPNH patient with *FLNI* gene mutation.

We observed many well-differentiated pyramidal neurons distributed randomly throughout the periventricular nodules (Fig. 2F, G). This morphology is similar to that of neurons in the cerebral cortex, rather than to those in the striatum, and this observation is consistent with that of Eksioğlu et al. [12]. We found that only a few small neurons showed immunoreactivity to the antibodies against the calcium-binding proteins calbindin, parvalbumin, and calretinin (Fig. 2H, I). Staining for the calcium-binding proteins identifies putative γ -aminobutyric acid (GABA)ergic neurons. It has been speculated that the epileptogenicity in cortical dysplasia, in some cases, is related to a decrease of the GABAergic interneurons and subsequent imbalance of excitation and inhibition in the foci of intractable epilepsy [44]. It is unclear whether seizure activity in our patient originated from the nodules in the deep cerebrum, and/or whether the number or function of the

inhibitory neurons was deficient. It seems more plausible that abnormal axonal connectivity (described below) might be associated with epileptogenesis. However, several other cellular and physiological aspects of cortical dysplasia that may be associated with epilepsy are known [46]. In the present case, precise mechanisms underlying epilepsy remain unclear.

We examined the characteristics of the fiber projections within and outside the nodules using DiI (Fig. 3). DiI [DiIC₁₈(3)] is one of the lipophilic carbocyanine dyes that can incorporate into cell membranes. Transfer of the dye between intact membranes is usually negligible. Therefore, DiI has been used in a variety of tracing applications, including anterograde and retrograde axonal projection study. We detected an apparent connection between the nodules and the surrounding white matter. The fibers exited through the myelinated indentation of the white matter (Fig. 2B) to form bundles (Fig. 3G), or extended directly across the margin of the nodule (Fig. 3H). We also demonstrated the possibility of a projection from the nodules to the cerebral cortex (Fig. 3K), although we failed to trace the whole length of the fiber path, and it is unclear whether the labeled axons were originating from (i.e., anterogradely labeled) or reached to (retrogradely labeled) the nodules. Hannan et al. [20] examined fiber projections using a similar DiI tracing technique in the brain tissues of four children with subcortical or periventricular nodular heterotopia. The cases were etiologically distinct from the BPNH cases, in that they all showed more severe malformation complexes in the brain. The connection between the nodules and the surrounding white matter is limited [20], and the profiles of fiber projection may differ according to the etiology. In this case, abnormal axonal circuits may have existed between the adjacent nodules and between the nodules and cerebral cortex. Studies using orthograde and retrograde tracers have revealed that heterotopic neurons in the *tish* rat, a neurological mutant exhibiting bilateral subcortical band heterotopia, project to appropriate subcortical sites and establish connections with the thalamus [39].

In the present case, a relatively large number of neurons were located close to the ventricle to form multiple nodules (Fig. 2B). On the other hand, the cortex on the convex and lateral sides appeared to be of normal thickness, and the number of cortical neurons did not appear to be reduced. This implies that a subset of young neurons failed to migrate completely, with the remainder migrating normally into the cortical plate. We did not observe an increased number of single heterotopic neurons within the white matter along the route taken by the migrating neurons. A cell-autonomous mosaic phenotype, with random activation/inactivation of the X chromosome, may regulate the behavior of the individual neurons and may also explain the morphological phenotype. Alternatively, the gene product might be involved in the regulation of neuron production or in the initial steps of the neurons propagating from the proliferating zones. In cross-sections of the cerebrum, we identified a border between the periventricular nodules and the caudate nucleus, where myelinated bundles from the white matter reached the ventricular surface (Fig. 2A, D).

Based on the location of the nodules, they appeared to have developed from the dorsolateral portion of the ventricular and subventricular zones, rather than from the ganglionic eminences. Disruption of the radial glial organization has been suggested to be responsible for some of the neuronal migration abnormalities observed in some autopsied fetuses with periventricular heterotopia [38] and neocortical tubers [35].

Filamin 1 protein promotes orthogonal branching of actin filaments [18, 19] and is important in coagulation and vascular development. Furthermore, Filamin 1 binds the intracellular domain of tissue factor, the protease receptor for coagulation factor VII, in association with actin filament reorganization [34]. The tissue factor has multiple roles in vascular development and angiogenesis [5, 34]. Mutation of the *FLN1* gene may, therefore, induce vascular anomalies. The high incidence of patent ductus arteriosus in these patients may relate to the role of Filamin 1 in vascular remodeling [16]. In the present case, widespread microvascular anomalies were present in the cerebral cortex (Fig. 4). In the development of the blood vessels, the arteries may have sprouted in a parallel manner. They lacked a properly configured tunica media (Fig. 4C, D, I), while the walls were labeled by the actin antibody with a variable intensity (Fig. 4F). This profile may be related to the presence of pericytes close to the walls (Fig. 4I), since this cell type possesses both muscle and non-muscle actins [26]. A network of basal lamina bounded by endothelial cells was seen in many lumina (Fig. 4E, G, I). Red blood cells were seen within many individual lumina (Fig. 4C), indicating blood circulation through them. We also found GFAP-labeled processes within the channels of vessel walls (Fig. 4H). The gliogenic period coincides with rapid growth of the blood vessels [6]. We speculate that processes of astrocytes invaded the channel during the courses of development of the blood vessels. They might have formed glia limitans that covered each individual vessel.

Widespread glomeruloid vascular changes were noted throughout the brain and spinal cord of fetal siblings with congenital hydrocephalus-hydrancephaly [14]. The features of the abnormal vessels in the hydrocephalic fetuses seem to be somewhat similar to those of glomeruloid vessels in the present case, but intracytoplasmic inclusions were observed in pericytes of the glomeruloids in the fetal brain. The etiology and pathological features of the brain are apparently distinct from those of the present case. Similar vascular alterations (namely glomerular-loop formations, vascular bundles, and vascular wickerworks) were also observed in a proportion of arterioles and precapillaries in many senile brains [1, 24, 25], and that may be associated with certain processes of aging. In the present case, it seems likely that a large proportion of parenchymal arteries branched off at the Virchow-Robin space and ran parallel throughout the cortex. The diameter of individual lumina of the glomeruloid vessels seems to be much smaller than that observed in the senile brains [24].

In addition to the microvascular anomaly, we noticed dysplastic cytoarchitecture in the cerebral cortex (Fig. 5). The distorted locations of neurons appeared to be associ-

ated with the malformed vessels. Even though our patient also suffered from intractable epilepsy, the characteristic features of the dysplastic cortex were distinct from those of cortical dysplasia observed in surgical specimens of a subset of patients with intractable epilepsy, which include increased cellularity of the molecular layer, persistent remnants of the subpial granular cell layer, marginal glioneuronal heterotopia, neuronal cytomegaly, and ballooned cells [31, 45]. The features of microvascular anomaly and dysplastic cortex are not likely to be common in patients with periventricular heterotopia; other autopsy cases with BPNH have not shown such changes [12, 38]. However, there is a possibility that a subset of patients with periventricular heterotopia suffer from vascular anomaly. The majority of patients with BPNH have normal intelligence [2, 11, 12, 36, 43], with only some being retarded [2]. Our patient was mentally retarded, which might be related to the observed widespread cortical dysplasia that was most apparent in the frontal cortex.

Acknowledgements The authors thank Jeffrey A. Golden, Department of Pathology, Children's Hospital of Philadelphia, Pa., USA, for reading of the manuscript and helpful comments. We also thank Dr. T. Morita, Department of Pathology, Shinrakuen Hospital, Niigata, Japan, for comments on the vessel alterations. We wish to express our appreciation to T. Hasegawa, S. Egawa, Y. Ohta, C. Tanda, J. Takasaki and K. Homma for technical assistance, and to M. Machida, K. Abe and T. Koike for help in preparing the manuscript. This work was supported in part by a grant (R00-011) from the Japan Epilepsy Research Foundation, a grant (12B-2) for Nervous and Mental Disorders from the Ministry of Health, Labor and Welfare, Japan, a grant for Medical Research from the Tsukada Foundation, Japan, and Grant-in-Aid (#12470287) from the Ministry of Education, Culture, Sports, Science, and Technology, Japan.

References

1. Akima M, Nonaka H, Kagesawa M, Tanaka K (1986) A study on the microvasculature of the cerebral cortex. Fundamental architecture and its senile change in the frontal cortex. *Lab Invest* 55:482-489
2. Barkovich AJ, Kjos BO (1992) Gray matter heterotopia: MR characteristics and correlation with developmental and neurologic manifestations. *Radiology* 182:493-499
3. Barkovich AJ, Jackson DE Jr, Boyer RS (1989) Band heterotopias: a newly recognized neuronal migration anomaly. *Radiology* 171:455-458
4. Borgatti R, Zucca C, Piccinelli P, Radice L, Tofani A, Benti R, Triulzi F (2000) Unilateral periventricular nodular heterotopia associated with diffuse areas of cerebral functional abnormalities. *J Child Neurol* 15:622-626
5. Bugge TH, Xiao Q, Kombrinck KW, Flick MJ, Holmbäck K, Danton MJS, Colbert MC, Witte DP, Fujikawa K, Davie EW, Degen JL (1996) Fatal embryonic bleeding events in mice lacking tissue factor, the cell-associated initiator of blood coagulation. *Proc Natl Acad Sci USA* 93:6258-6263
6. Caley DW, Maxwell DS (1970) Development of the blood vessels and extracellular spaces during postnatal maturation of rat cerebral cortex. *J Comp Neurol* 138:31-48
7. Canapicchi R, Padolecchia R, Puglioli M, Collavoli P, Marcella F, Valleriani AM (1990) Heterotopic gray matter. Neuro-radiological aspects and clinical correlations. *J Neuroradiol* 17:277-287
8. Cho WH, Seidenwurm D, Barkovich AJ (1999) Adult-onset neurologic dysfunction associated with cortical malformations. *AJNR* 20:1037-1043

9. Dobyns WB, Andermann E, Andermann F, Czapansky-Beilman D, Dubeau F, Dulac O, Guerrini R, Hirsch B, Ledbetter DH, Lee NS, Motte J, Pinard J-M, Radtke RA, Ross ME, Tampieri D, Walsh CA, Truwit CL (1996) X-linked malformations of neuronal migration. *Neurology* 47:331-339
10. Dobyns WB, Guerrini R, Czapansky-Beilman DK, Pierpont MEM, Breningstall G, Yock DH, Bonanni P, Truwit CL (1997) Bilateral periventricular nodular heterotopia with mental retardation and syndactyly in boys: a new X-linked mental retardation syndrome. *Neurology* 49:1042-1047
11. Dubeau F, Tampieri D, Lee N, Andermann E, Carpenter S, Leblanc R, Olivier A, Radtke R, Villemure JG, Andermann F (1995) Periventricular and subcortical nodular heterotopia. A study of 33 patients. *Brain* 118:1273-1287
12. Eksioglu YZ, Scheffer IE, Cardenas P, Knoll J, DiMario F, Ramsby G, Berg M, Kamuro K, Berkovic SF, Duyk M, Parisi J, Huttenlocher PR, Walsh CA (1996) Periventricular heterotopia: an X-linked dominant epilepsy locus causing aberrant cerebral cortical development. *Neuron* 16:77-87
13. Fink JM, Dobyns WB, Guerrini R, Hirsch BA (1997) Identification of a duplication of Xq28 associated with bilateral periventricular nodular heterotopia. *Am J Hum Genet* 61:379-387
14. Fowler M, Dow R, White TA, Greer CH (1972) Congenital hydrocephalus-hydroencephaly in five siblings, with autopsy studies: a new disease. *Dev Med Child Neurol* 14:173-188
15. Fox JW, Walsh CA (1999) Periventricular heterotopia and the genetics of neuronal migration in the cerebral cortex. *Am J Hum Genet* 65:19-24
16. Fox JW, Lamperti ED, Eksioglu YZ, Hong SE, Feng Y, Graham DA, Scheffer IE, Dobyns WB, Hirsch BA, Radtke RA, Berkovic SF, Huttenlocher PR, Walsh CA (1998) Mutations in filamin 1 prevent migration of cerebral cortical neurons in human periventricular heterotopia. *Neuron* 21:1315-1325
17. Friede RL (1989) Developmental neuropathology, 2nd edn. Springer, New York Berlin Heidelberg, pp 333-335
18. Glogauer M, Arora P, Chou D, Janmey PA, Downey GP, McCulloch CAG (1998) The role of actin-binding protein 280 in integrin-dependent mechanoprotection. *J Biol Chem* 273:1689-1698
19. Gorlin J, Yamin R, Egan S, Stewart M, Sossel T, Kwiatkowski D, Hartwig J (1990) Human endothelial actin-binding protein (ABP-280, nonmuscle filamin): a molecular leaf spring. *J Cell Biol* 111:1089-1105
20. Hannan AJ, Servotte S, Katsnelson A, Sisodiya S, Blakemore C, Squier M, Molnár Z (1999) Characterization of nodular heterotopia in children. *Brain* 122:219-238
21. Hartwig J (1992) Mechanisms of actin rearrangements mediating platelet activation. *J Cell Biol* 106:1525-1538
22. Hartwig J, Shevlin P (1986) The architecture of actin filaments and the ultrastructural location of actin-binding protein in the periphery of lung macrophages. *J Cell Biol* 103:1007-1020
23. Hartwig J, Tyler J, Stossel T (1980) Actin-binding protein promotes the bipolar and perpendicular branching of actin filaments. *J Cell Biol* 87:841-848
24. Hassler O (1965) Vascular changes in senile brains. A microangiographic study. *Acta Neuropathol (Berl)* 5:40-53
25. Hassler O (1967) Arterial deformities in senile brains. The occurrence of the deformities in a large autopsy series and some aspects of their functional significance. *Acta Neuropathol (Berl)* 8:219-229
26. Herman IM, D'Amore PA (1985) Microvascular pericytes contain muscle and nonmuscle actins. *J Cell Biol* 101:43-52
27. Huttenlocher PR, Taravath S, Mojtahedi S (1994) Periventricular heterotopia and epilepsy. *Neurology* 44:51-55
28. Jan MMS (1999) Outcome of bilateral periventricular nodular heterotopia in monozygotic twins with megalencephaly. *Dev Med Child Neurol* 41:486-488
29. Li LM, Dubeau F, Andermann F, Fish DR, Watson C, Cascino GD, Berkovic SF, Moran N, Duncan JS, Olivier A, Leblanc R, Harkness W (1997) Periventricular nodular heterotopia and intractable temporal epilepsy: poor outcome after temporal lobe resection. *Ann Neurol* 41:662-668
30. Matsudaira P (1994) Actin crosslinking proteins at the leading edge. *Semin Cell Biol* 5:165-174
31. Mischel PS, Nguyen LP, Vinters HV (1995) Cerebral cortical dysplasia associated with pediatric epilepsy. Review of neuropathologic features and proposal for a grading system. *J Neuropathol Exp Neurol* 54:137-153
32. Moro F, Carrozzo R, Veggiotti P, Tortorella G, Toniolo D, Volzone A, Guerrini R (2002) Familial periventricular heterotopia: missense and distal truncating mutations of the FLN1 gene. *Neurology* 58:916-921
33. Oda T, Nagai Y, Fujimoto S, Sobajima H, Kobayashi M, Togari H, Wada Y (1993) Hereditary nodular heterotopia accompanied by mega cisterna magna. *Am J Med Genet* 47:268-271
34. Ott I, Fischer EG, Miyagi Y, Mueller BM, Ruf W (1998) A role for tissue factor in cell adhesion and migration mediated by interaction with actin-binding protein 280. *J Cell Biol* 140:1421-1253
35. Park S-H, Pepkowitz SH, Kerfoot C, De Rosa MJ, Poukens V, Wienecke R, DeClue JE, Vinters HV (1997) Tuberous sclerosis in a 20-week gestation fetus: immunohistochemical study. *Acta Neuropathol* 94:180-186
36. Poussaint TY, Fox JW, Dobyns WB, Radtke R, Scheffer IE, Berkovic SF, Barnes PD, Huttenlocher PR, Walsh CA (2000) Periventricular nodular heterotopia in a patient with filamin-1 gene mutations: neuroimaging findings. *Pediatr Radiol* 30:748-755
37. Raymond AA, Fish DR, Stevens JM, Sisodiya SM, Alsanjari N, Shorvon SD (1994) Subependymal heterotopia: a distinct neuronal migration disorder associated with epilepsy. *J Neurol Neurosurg Psychiatry* 57:1195-1202
38. Santi MR, Golden JA (2001) Periventricular heterotopia may result from radial glial fiber disruption. *J Neuropathol Exp Neurol* 60:856-862
39. Schottler F, Couture D, Rao A, Kahn H, Lee KS (1998) Subcortical connections of normotopic and heterotopic neurons in sensory and motor cortices of the *tish* mutant rat. *J Comp Neurol* 395:29-42
40. Sheen VL, Dixon PH, Hong SE, Fox JW, Kinton L, Sisodiya SM, Duncan JS, Dubeau F, Scheffer IE, Schachter SC, Wilner A, Henchy R, Crino P, Kamuro K, DiMario F, Berg M, Kuzniecky R, Cole AJ, Bromfield E, Biber M, Schomer D, Wheless J, Silver K, Mochida GH, Berkovic SF, Andermann F, Andermann E, Dobyns WB, Wood NW, Walsh CA (2001) Mutations in the X-linked filamin 1 gene cause periventricular nodular heterotopia in males as well as in females. *Hum Mol Genet* 10:1775-1783
41. Sisodiya SM, Free SL, Thom M, Everitt AE, Fish DR, Shorvon SD (1999) Evidence for nodular epileptogenicity and gender differences in periventricular nodular heterotopia. *Neurology* 52:336-341
42. Sisodiya SM, Free SL, Duncan JS, Stevens JM (2000) Bilateral periventricular and subcortical heterotopia in a man with refractory epilepsy. *Epilepsia* 41:352-354
43. Smith AS, Weinstein MA, Quencer RM, Muroff LR, Stonesifer KJ, Li FC, Wener L, Soloman MA, Cruse RP, Rosenberg LH, Berke JP (1988) Association of heterotopic gray matter with seizures: MR imaging. Work in progress. *Radiology* 168:195-198
44. Spreafico R, Battaglia G, Arcelli P, Andermann F, Dubeau F, Palmieri A, Olivier A, Villemure J-G, Tampieri D, Avanzini G, Avoli M (1998) Cortical dysplasia. An immunocytochemical study of three patients. *Neurology* 50:27-36
45. Taylor DC, Falconer MA, Bruton CJ, Corsellis JAN (1971) Focal dysplasia of the cerebral cortex in epilepsy. *J Neurol Neurosurg Psychiatry* 34:369-387
46. Vinters HV, Park SH, Johnson MW, Mischel PS, Catania M, Kerfoot C (1999) Cortical dysplasia, genetic abnormalities and neurocutaneous syndrome. *Dev Neurosci* 21:248-259
47. Watson C, Nielsen SL, Cobb C, Burgerman R, Williamson B (1996) Pathological grading system for hippocampal sclerosis: correlation with magnetic resonance imaging-based volume measurements of the hippocampus. *J Epilepsy* 9:56-64